Proceedings of the Fourth IASTED International Conference
POWER AND ENERGY SYSTEMS (AsiaPES 2008)
April 2-4, 2008 Langkawi, Malaysia
ISBN CD: 978-0-88986-732-1

DESIGN AND IMPLEMENTATION OF A HYBRID POWER GENERATION SYSTEM WITH FUEL CELLS AND BATTERIES

Chih-Chiang Hua Wun-Cin Syu
National Yunlin University of Science and Technology Department of Electrical Engineering 123 University load, Section 3, Douliou, Yunlin, Taiwan, R.O.C
HUACC@yuntech.edu.tw g9512704@yuntech.edu.tw

ABSTRACT
A soft-switching method and control scheme for an isolated step-up full bridge converter is proposed in this paper to implement a hybrid power generation system with Fuel Cells and Batteries. By using leakage inductance of the transformer, the system conversion efficiency can be improved and a simple control is achieved. Adding clamping-diodes in series with leading-leg can greatly lessen the ringing of the transformer and filter diodes. The system consists of three power stages, including a bi-directional DC-DC converter, a ZVS-FB DC/DC converter, and a DC/AC inverter. The DC/AC inverter is used to transfer the power for ac applications ($110V_{rms}$ /60Hz). Due to the PEMFC cannot respond quickly, its output voltage is easily affected by load variations and polarization loss. The bi-directional converter with flexible control strategy can provide power sharing and energy storage at different conditions of the load, which makes its suitable for PEMFC powered AC applications. In this paper, the tested results will be presented to verify the performance of the system.

KEY WORDS
PEMFC, soft-switching method, Fuel Cell, hybrid power generation system

1. Introduction

Fuel cells are considered to be one of the most promising future energy generation devices, because of their various advantages such as high energy efficiency, low operation noise, low emission, environmental friendliness and the ability to generate electricity directly, etc [1], [2]. Major applications were identified in various areas such as transportation, stationary power, and portable power. The hydrogen and oxygen pass through the proton exchange membrane and execute chemical reaction to produce electricity. The exchange membrane cannot respond quickly when the load changes. So it needs to use power converter to compensate the load variations appropriately. Fig. 1 shows the typical layout of the system configuration including: (1) a bi-directional DC-DC converter between fuel cells and batteries, (2) an isolated DC/DC converter to be able to boost the low voltage (22~42 V) of the fuel cell to a dc link voltage high enough (200 V) and (3) a subsequent DC/AC conversion by the inverter to obtain utility type ac voltage (110-V_{rms} at 60 Hz).

Owing to regulating the bi-directional power flow appropriately, the flexible control strategy is applied in the bi-directional DC-DC converter that connects the batteries and fuel cell to supply active compensation for fuel cell energy management and load allotment. In this system, the batteries are needed to release or store energy instantaneously and compensate the fuel cell during dynamic conditions. The important part is to control the timing of charging or discharging, and accomplish the type of the energy management using power electronic technologies.

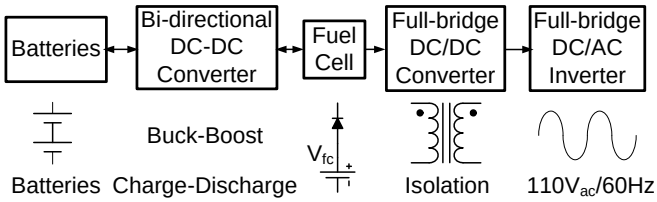

Figure 1. The typical layout of the system configuration

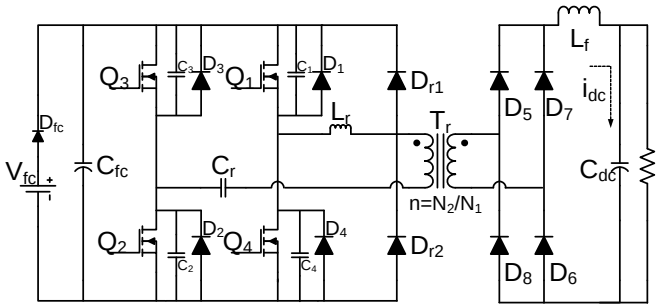

Figure 2. Topology of the proposed full-bridge converter

Finally, the system integrate bi-directional DC-DC converter with DSP (TMS320LF2407A) to achieve the adjustment of power flow, active distribution, and energy storage between fuel cell and battery.

A step-up converter can be used to boost the low voltage to high (200 V), but the higher duty ratio a boost converter has, the lower efficiency it is. The efficiency of a boost converter for such an application is approximately 40% [3]. Push–pull, half-bridge, and full-bridge converters can also be used to boost the low voltage of the

fuel cell to the required level [4], [5]. However, these converters have large turns ratios (such as 1:20) of the isolated transformers. Therefore, large leakage inductances cause duty cycle loss, low energy efficiency and difficulty in control of the dc-dc converter [6]. For high-power applications, the full-bridge (FB) zero-voltage-switching (ZVS) PWM converter shown in Fig. 2 is the most widely used circuit, which can achieve ZVS for active power switches on the primary side of the transformer in a wide range of load current and input voltage with reduced circulating energy and conduction losses [7-11].

The proposed full-bridge converter uses the leakage inductance of the transformer to help energy conversion, which ot only promotes the conversion efficiency, but also mitigates difficulty in control. The full-bridge converter employ voltage clamping diodes (D_{r1}, D_{r2}) in primary side of transformer having some merits as follows: (1) it can reduce unreasonable transient characteristic of high-frequency transformer efficiently, (2) diminish electromagnetic interference (EMI), and (3) slow down the phenomenon of voltage spike, ringing and current ringing in primary side of transformer. (4) The circuit frame is simple and not influences the analysis of power circuit. (5) The rate of forward current in clamping diode is small and low power losses. To help retard the voltage stress of power switches and output diodes. Moreover, the output side of the ZVS-FB converter is connected to the input side of the single phase inverter, which provides a fixed 110 VAC by the SPWM control.

2. Topologies and circuit operations

The bi-directional DC-DC converter has two parts to cascade shown in Fig. 3. One is the buck converter, and the other is the boost converter. The function of the bi-directional converter is to charge or discharge batteries and adjusts the power flow in different situation. The operation modes are as follows: At beginning, programs set the maximum output current of the fuel cell. When the output current of the fuel cell is less than the level of the setting, the converter is operated in buck mode to charge batteries. The charging method is CC-CV (constant current-constant voltage) with two batteries in series (24 V) and provides power to loads. If the charging current of batteries is less than the minimum setting current, the charging mode will stop to protect batteries overcharging. If the load demand is higher than the setting value, the fuel cell current will be limited and the remained current will be compensated by the bi-directional converter in boost mode. If the voltage of batteries lowers to the setting volt, continuous discharging may spoil batteries. To avoid destruction of batteries, programs will shutdown the system.

The operation waveforms of the zero-voltage-switching full-bridge DC/DC converter are shown in Fig. 4. which adopts pulse width modulation to adjust the output power. The responsible duty ratio uses $D_2 = 1 - D_1$, and $0 \leqq D_1 < 0.5$. When the triangular waveform (V_{tri}) is lower than D_1, power switch Q_1 turns on. When V_{tri} is higher than D_2, Q_3 turns on. As a result of the power MOS (Q_1, Q_2) or (Q_3, Q_4) must conduct simultaneously that the energy just can through high-frequency transformer produce output power to load. To facilitate the explanation of the circuit in Fig. 2, Fig. 5 shows its simplified circuit diagram. It is assumed that the inductance of output filter L_f is large enough so that during a switching cycle the output filter can be modeled as a constant current source with a magnitude equals to output current i_{dc}.

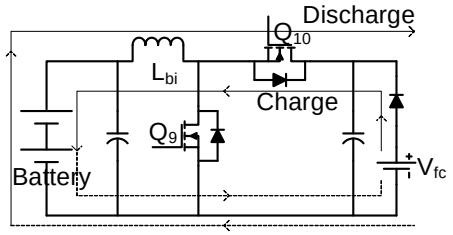

Figure 3. The bi-directional DC-DC converter

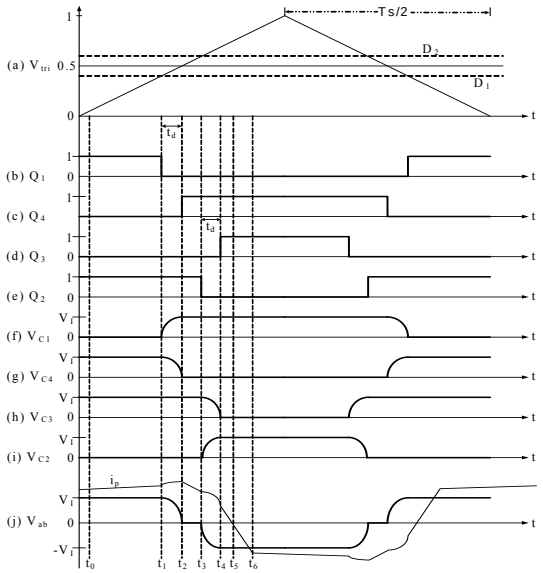

Figure 4. The control signal of ZVS-FB DC/DC converter

The operation of the converter during different time periods in the first half cycle is explained as follows.

2.1 Interval [t_0~t_1]: Energy transferring mode

Switches Q_1, and Q_2 are gated. A closed current path is created as shown in Fig. 5(a). Diodes of filter D5, D6 are in conduction state. The energy store in resonant inductor (L_r) and the leakage inductance of the transformer (L_{leak}) by transformer transfer power to load. One can derive that $V_P = V_I$, $V_S = V_O$.

$$V_L = V_P - V_S = V_I - V_O \quad (1)$$

$$I_L = \frac{V_I - V_O}{L} t \quad (2)$$

2.2 Interval [t_1~t_2]: First resonant mode

At this moment, Q_1 is turned off. According to Faraday Lentz Law, current i_p in the inductor must keep continuously, so it charges capacitor C_1 to V_I and discharge capacitor C_4 to zero at the same rate. After capacitor C_4 is fully discharged, i.e., when voltage V_{Q4} reaches zero, current i_p starts flowing through antiparallel diode D_4 of switch Q_4, as shown in Fig. 5(b).

$$V_{C1}(t) = V_{C4}(t) + V_I \tag{3}$$

2.3 Interval [t_2~t_3]: Energy storing mode

To achieve zero-voltage turn-on of switch Q_4, it is necessary to turn on switch of Q_4 while its antiparallel diode D_4 is conducting. In Fig. 5(C), the power switch Q_4 is turned on immediately after voltage V_{Q4} has fallen to zero which can eliminate switching loss of power MOS Q_4. The output power is supplied by capacitor C_{dc}.

2.4 Interval [t_3~t_4]: Second resonant mode

When switch Q_2 is turned off. According to Faraday Lentz Law, current i_p in the inductor must keep continuously, which initiates the charging of capacitance C_2 of switch Q_2 and discharging of capacitance C_3 of switch Q_3, as shown in Fig.5(d). Also, C_2 is charged to V_I and its opposite capacitor C_3 is discharged to zero.

$$V_{C2}(t) = V_{C3}(t) + V_I \tag{4}$$

2.5 Interval [t_4~t_5]: Energy reverse mode

This topological stage ends at t = t_5 when voltage V_{Q3} across switch Q_3 reaches to zero and antiparallel diode D_3 of switch Q_3 starts conducting current, as shown in Fig.5(e). To achieve ZVS of switch Q_3, switch Q_3 needs to be turned on while diode D_3 is conducting that can reduce switching loss of transistor Q_3. At that moment, $n \times i_{dc}$ equals to zero.

2.6 Interval [t_5~t_6]: Energy transferring mode

When switch Q_3 is completely turned on, the current i_p flows inversely direction path so that the circuit enters the same topological stage as shown in Fig. 5(f), awaiting the next switching cycle to be initiated by the controller.

It should be noted that, in the proposed circuit, clamping diodes have no effect on commutation time of the primary current from one direction to the other. This commutation time is proportional to the sum of leakage inductance of the transformer T_r and resonant inductor L_r, because they are effectively in series with the power path. Therefore, to minimize the duty cycle loss and optimize the performance of the circuit, it is necessary to minimize the leakage inductance of transformer T_r and resonant inductor L_r. In this paper, the control strategy and adding a set of clamping diode can efficiently restrain parasitic-ringing energy of power switches, which further improves the circuit performance particularly in light load.

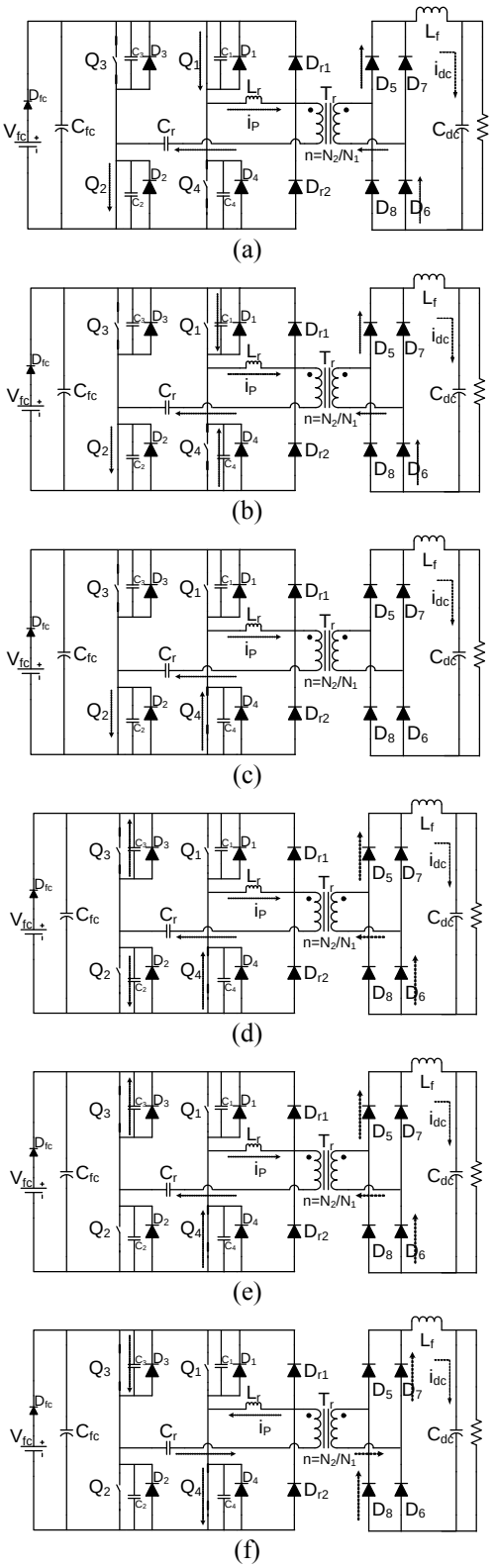

Figure 5. Operation modes of ZVS-FB DC/DC converter

In this paper, the DC/AC inverter uses a full bridge inverter frame through low power filter to provide a fixed

voltage and frequency of the single phase power. The power circuit of inverter is shown in Fig. 6.

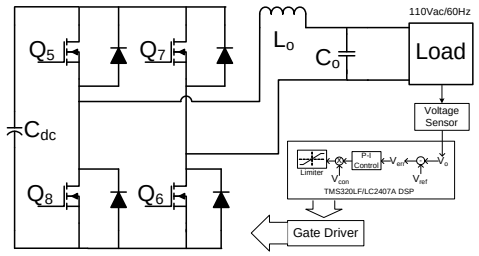

Figure 6. The full-bridge DC/AC inverter.

In most control method of the inverter, the technique of SPWM (sinusoidal pulse width modulation) is usually adopted for the time being. Using this method can acquire stable output voltage and low harmonic distortion. Single-pole voltage switching method is adopted in this inverter and its switching frequency is twice the double-pole voltage switching, so its harmonic content is lower than double-pole switching. Therefore, the design of filter circuit can reduce dimension and weight to obtain the same purpose. According to (5) and (6), inverter can decide the size of the output filter to attain the optimal dynamic response and suppress the output distortion.

$$L_f \geq \frac{V_L \times T_S}{\Delta I_{L\_\max}} \tag{5}$$

$$C_f \geq \frac{T_S \times \Delta I_{L\_\max}}{2 \times \Delta V_O} \tag{6}$$

3. Control strategies

3.1 Control strategy of the bi-directional DC-DC converter

According to the control flow-chart of bi-directional DC-DC converter in Fig. 7. Eq. (7)shows the duty cycle of the bi-directional DC-DC converter with P-I controller building in a DSP. The control strategy of batteries is divided into two parts. Particularly, the control strategy uses protecting batteries and the system to make sure the safety in all components. The charging mode and discharging mode are shown as follows:

$$d_{new} = d_{old} + k_p * error + k_i * \int error \cdot dt \tag{7}$$

3.1.1 Buck/Charging mode

In the charging mode, the charging strategy adopts CC-CV (constant current-constant voltage) method. In the beginning, the controller gets feedback signals of the voltage and current from batteries, using the command of charging voltage/current via the P-I equation get the error value in eq. (7). The proportional and integral terms of the errors are actually through gating power MOS compensating the change of the duty cycle Δd at variety of current/voltage of batteries.

3.1.2 Boost/Discharging mode

In the discharging mode, the bi-directional converter operates in boost mode to compensate power. At first, the DSP gathers the feedback signals of the current from batteries and DC bus voltage. The command of discharging current through the P-I equation get the error value in eq. (7). The DSP deliver duty cycle signals to gate the power switches compensating the remained energy.

At any time, the control strategy selects only one regulation mode and then the bi-directional DC-DC converter works only one control objective.

3.2 Control strategy of the zero-voltage-switching full-bridge DC/DC converter

The control equation (8) of the ZVS-FB DC/DC converter is as follows:

In order to regulate the DC bus voltage, the ZVS-FB converter is controlled as a PS-PWM. φ is the phase angle of Q_1. The $0 \leqq D_1 < 0.5$ equals to $0 \leqq \varphi < 180°$. Using P-I control strategy multiplies the error value of V_{dc} to get duty cycle of D_1. The larger pulse width is, the more power output energy is, i.e., the converter can transfer more power to load; on the contrary, the energy that is transferred to output load is less. By modulating the responsibility of duty cycle (D_1, D_2); for the purpose of adjusting the output energy, the full-bridge converter can regulate the net output power in the variety of load.

$$\begin{aligned} error\_value\_V_{dc} &= V_{dc,old} - V_{dc,new} \\ D_1 &= G_{P-I} * error\_value\_V_{dc} \end{aligned} \tag{8}$$

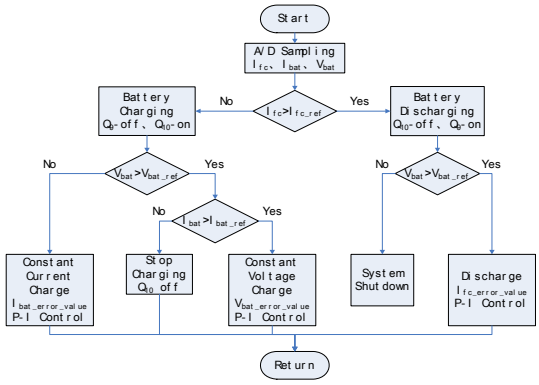

Figure 7. The control flow-chart of bi-directional DC-DC converter

3.3 Control strategy of full-bridge DC/AC inverter

The Control framework diagram of this circuit is shown in Fig. 6, using a full bridge inverter frame. The SPWM technique and the control of voltage feedback signals are used in this paper. At first, the DSP feed-backs output voltage and establish a sinusoidal function table to obtain

the reference signal. The above two values are compared and the error value V_{err} is obtained. The PI control is implemented on the DSP, and a sinusoidal control signal V_{con} is compared with a triangle wave signal V_{tri}. The switching method adopts high/low frequency to gate the power switches, i.e., the circuit of left-leg (Q_5, Q_8) operates in high frequency (20 kHz) and the right-leg (Q_7, Q_6) operates in low frequency (60 Hz) to acquire utility type AC voltage (110-V rms at 60 Hz).

4. Experimental verification

The performance of the proposed circuit was verified on a 1kW (continuous 740 W and compensated 240 W) experimental prototype operating at 20 kHz. The experimental converter was designed to operate from 22~42V input and delivers 3.7A from a 200V output. To cascade a DC/AC inverter produce 110 V_{rms} at 60 Hz for AC applications. The experimental circuit is shown in Fig. 8. The control circuit of the bi-directional DC-DC converter, ZVS-FB converter and single phase inverter was implemented using a digital signal processor.

Fig. 8 shows the oscillogram of key waveforms of the bi-directional DC-DC converter. The circuit uses two lead-acid batteries in series (24V/26Ah). From top to bottom presents the voltage of fuel cell (V_{fc}), voltage of batteries (V_{bat}), current of fuel cell (I_{fc}), and current of batteries (I_{bat}). As can be seen from Fig. 8, the bi-directional converter operates in charging/discharging mode to verify the performance of circuit and the timing of charging/discharging mode depends on the limit value of the fuel cell output current. The fuel cell provides current of about 6A, supplying 2A to the load and charging the batteries in CC mode at the same time. When the batteries voltage reaches the voltage limit (28.6 V), CV mode applies and the batteries voltage is regulated. In this mode, the charging current of batteries and the output current of fuel cell decreases. So the voltage of fuel cell rises gradually. In charging-stop mode, the charging current of batteries decreases to 0.05C (1.3A) and the switch of charge Q_{10} will be turned off to avoid the batteries overcharging. When the load demands higher power, DC mode applies again. Later, the regulation mode changes in the following order: from DC, to CC, CV, Charging-stop, and back to DC mode. It is seen that the regulation mode is selected correctly and the fuel cell current, battery current and battery voltage were regulated properly.

To verify this new topology, a prototype unit is built and tested. Fig. 9 illustrates the prototype of the fuel cell generation system. This unit is rated at 1 kW owing to the current limitation on power device pins. It consists of three major parts: a bi-directional DC-DC converter board, a ZVS-FB DC/DC converter board, and a DC/AC inverter board. In this test unit, the switches of the fuel cell system are controlled by the same reference signal. Thus, for zero-voltage-switching full-bridge converter, the PS modulation angles between two legs for each phase are identical. This timing is critical; if it is slightly unmatched, it may cause large circulating energy among the transformer primary sides.

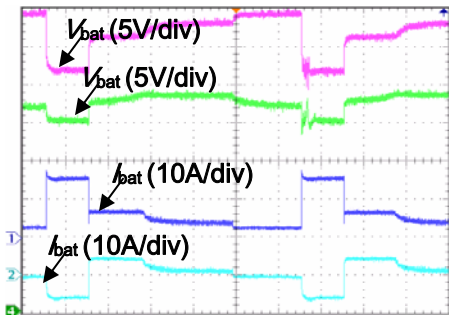

Figure 8. The key waveforms of bi-directional DC-DC converter

Fig. 10 shows the actual conversion ratio for the prototype. As can be seen, the experimental results match with the ideal ratio very closely. The discrepancy is the power loss in the circuit, caused by the impact of dead-time control in the leg switches and duty-cycle loss caused by circuit inductance. The experimental results also verify the converter soft switching operation. Device switching waveforms are shown in Fig. 11. All the devices turn ON without ZVS, as illustrated in Fig. 11(a). Fig. 11(b) shows the turn ON switching waveforms for the power switches devices with ZVS. It should be noticed that an increased load is good for achieving device ZVS operation. These ZVS waveforms for the leading-leg and lagging-leg are acquired with only 8% load condition. In Fig. 12, it is obviously to tell the difference between high-frequency transformer without using a set of clamping-diode and adopting it. Adding the clamping-diode can reduce the phenomenon of voltage spike and ringing to help restrain the problem of dynamic losses and electromagnetic interference that also can increase the life of all the components. As shown in Fig. 13, the ringing of the output filter diodes are suppressed by the clamping-diode. Hence, the effectiveness can be the same with previous descriptions. The zero-voltage-switching and clamping-diode discussed above improves system efficiency.

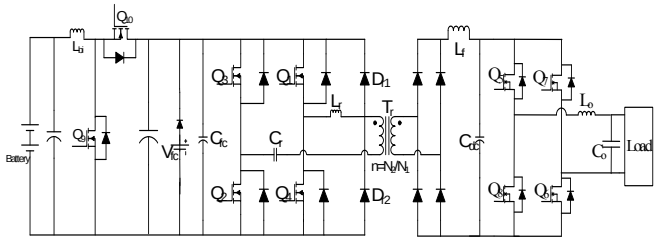

Figure 9. The prototype of the fuel cell generation system.

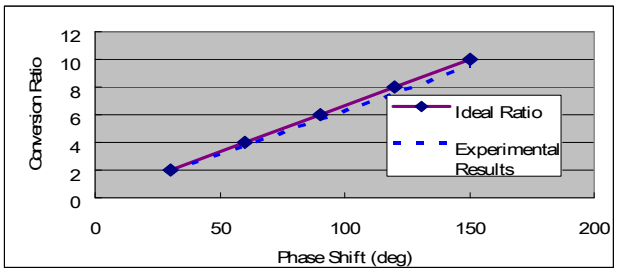

Figure 10. The conversion ratio for the prototype

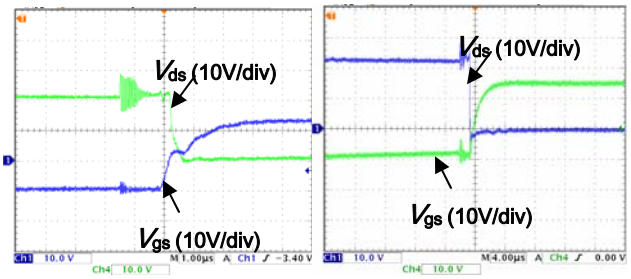

(a) (b)

Figure 11. The experimental waveforms of power switches. (a) without ZVS.(b) with ZVS

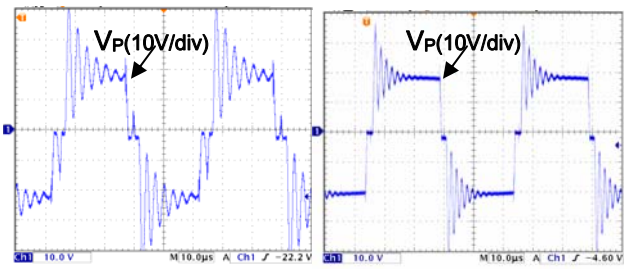

(a) (b)

Figure 12. The ringing waveforms of the high-frequency transformer. (a) without clamping-diodes. (b) with clamping-diodes

Experimental results for the isolated full-bridge boost mode are shown in Fig. 14. The load changes from 80W, 180W, 320W, 520W to 740W and its output voltage holds 200V in the range of the rated loads. The voltage of device is very clean, resulting in low voltage stress. Here, 200V is used to generate a $110V_{rms}$ inverter ac output. The dynamic operations of the single phase inverter are shown in Fig15, in which the load changes from 420 W to 1kW and from 1kW to 420W. Fig 15(a) shows the critical condition; one can see that the batteries compensate the power through bi-directional converter to load for ac applications. If the system operates below 740W, i.e., the fuel cell has spare energy to charge the batteries with CC-CV strategy as shown in Fig15(b). Furthermore, the hybrid fuel cell generation system is much useful than one fuel cell generation system to supply power for applications.

By comparing these experimentally obtained results with the analyzed waveforms in Fig. 4, the experimental results verify the proposed system. Research is going on to further reduce the cost and improve the energy efficiency of the hybrid fuel cell generation system.

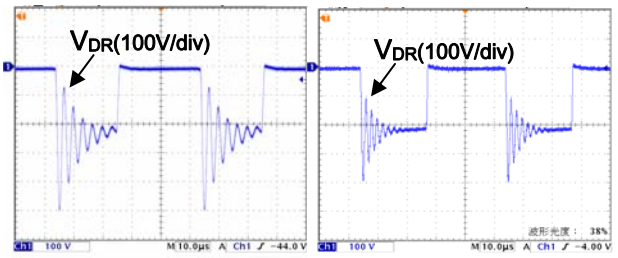

(a) (b)

Figure 13 The ringing waveforms of the output filter diodes . (a) without clamping-diodes. (b) with clamping-diodes

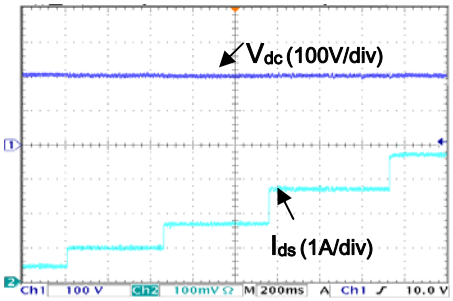

Figure 14. The variation waveform of the ZVS-FB converter

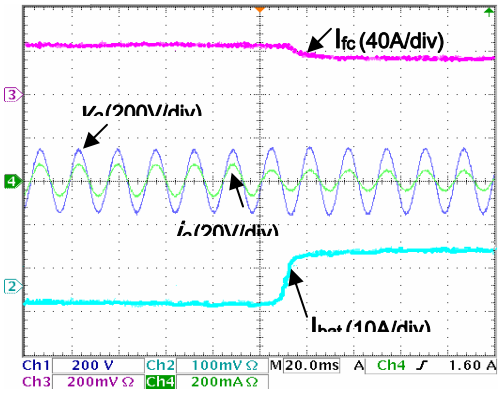

(a)

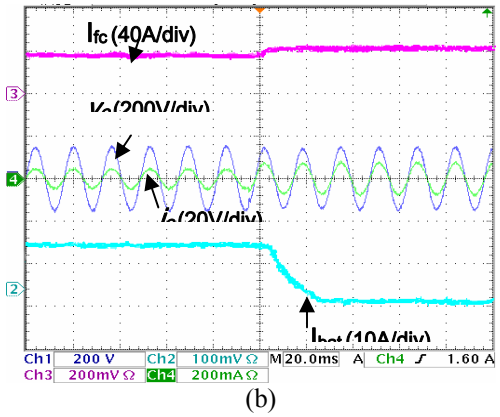

(b)

Figure 15. Dynamic waveforms of the hybrid system. (a)from 1k W to 420W. (b) from 420W to 1kW

5. Conclusion

The rated 1kW of a hybrid power fuel cell generation system is proposed. This paper presents a soft-commutating-method and control scheme to implement an isolated step-up converter, in which using leakage inductance of the transformer to help for energy conversion. This can improve the low efficiency and difficulty in control, resulting from the leakage inductance. A set of clamping-diode is used to mitigate the ringing of the transformer and output filter diodes. The merits make the converter operate in low temperature and low voltage stress caused by the low efficiency and the ringing. A soft-commutating criterion is discussed in this paper. Zero-voltage-switching is achieved for the switches of the full-bridge converter that can efficiently reduce the switching losses. The system can operate in a continuous 740W and peak 1kW was built using a PEMFC with the voltage range 22~42V and two 26Ah lead-acid batteries in series with nominal voltage 24V, respectively. Discussion about design and control issue of the system, including a bi-directional DC-DC converter, a ZVS-FB DC/DC converter, and a DC/AC inverter can be found in previous descriptions, in which the tested results are provided to verify the control design and transient response of the system.

References

[1] EG&G Technical Services, Inc. Science Applications International Corporation, *Fuel Cell Handbook*, 7th ed. Morgantown, WV: U.S. Dept. of Energy, Office of Fossil Energy, National Energy Technology Laboratory, Nov. 2004.

[2] H. B. Puttgen, P. R. MacGregor, and F. C. Lambert, "Distributed generation: Semantic hype or the dawn of a new era," *IEEE Power Energy*, vol. 1, no. 1, pp. 22–29, Jan./Feb. 2003.

[3] D. W. Hart, *Introduction to Power Electronics*, 1st ed. Englewood Cliffs, NJ: Prentice-Hall, 1997, pp. 213–214.

[4] *Fuel Cell Handbook*, 6th ed. Washington, DC: U.S. Department of Energy, Nov. 2002, DOE/NETL-2002/1179.

[5] H. Li, F. Z. Peng, and J. S. Lawler, "Anatural ZVS medium-power bidirectional DC-DC converter with minimum number of devices," *IEEE Trans. Ind. Appl.*, vol. 39, no. 2, pp. 525–535, Mar./Apr. 2003.

[6] J. Wang, F. Z. Peng, J. Anderson, A. Joseph, and R. Buffenbarger, "Low cost fuel cell inverter system for residential power generation," in *Proc. IEEE/APEC*, Anaheim, CA, Feb. 22–26, 2004, vol. 1, pp. 337–367.

[7] X. Ruan and Y. Yan, "A Novel Zero-Voltage and Zero-Current-Switching PWM Full-Bridge Converter Using Two Diodes in Series With the Lagging Leg," *IEEE Trans. Industry. Electronics*, vol. 48, no. 4, pp. 777-785, Aug. 2001,

[8] C. Liu, A. Johnson, and J. S. Lai, "A Novel Three-Phase Soft-Switched DC/DC Converter for Low-Voltage Fuel Cell Applications," *IEEE. Trans. Industry Applications*., vol. 41, no. 6, pp. 1691-1697, Nov/Dec. 2005.

[9] R. Sharma and H. Gao, "Low Cost High Efficiency DC-DC Converter for Fuel Cell Powered Auxiliary Power Unit of a Heavy Vehicle," *IEEE Trans. Power Electronics*., vol. 21, no. 3, pp. 587-591, May. 2006.

[10] Y. Jang, M. M. Jovanovic, and Y. M. Chang, "A New ZVS-PWM Full-Bridge Converter," *IEEE Trans. Power Electronics*., vol. 18, no. 5, pp. 1122-1126, Sept. 2003.

[11] L. Zhu, "A Novel Soft-Commutating Isolated Boost Full-Bridge ZVS-PWM DC-DC Converter for Bidirectional High Power Applications," *IEEE Trans. Power Electronics*., vol. 21, no. 2, pp. 422-427, Mar. 2006.